Diagrammatic approach in the variational coupled-cluster method

Y. Xian
School of Physics and Astronomy, The University of Manchester, Manchester M13 9PL, United Kingdom
(Received 7 June 2005; revised manuscript received 25 October 2005; published 30 December 2005)

We present an alternative approach based on a diagrammatic technique to the recently proposed variational coupled-cluster method. We apply this method to quantum antiferromagnetic bipartite lattices. In our analysis, infinite resummations of diagrams can be done in a straightforward manner. One such resummation reproduces spin-wave theory (SWT). Approximations beyond SWT can also be easily made. Interestingly, one such approximation produces a convergent, precise number for the order parameter of the one-dimensional isotropic model, in contrast to the well-known divergence of SWT; it also produces improved results for the two-dimensional square-lattice system. We also discuss relations and a possible combination of our approach with other established many-body theories.

DOI: 10.1103/PhysRevB.72.224438 PACS number(s): 75.10.Jm, 31.15.Dv

I. INTRODUCTION

A microscopic quantum many-body theory is mainly to study correlations between the constituent particles of a quantum system. The method of correlated basis functions[1] (CBFs) and the coupled-cluster method[2–4] (CCM) are two typical many-body theories which deal directly with wave functions. The CBF method has proved to be one of very few many-body theories capable of dealing with strongly correlated boson systems in the liquid phase such as the helium-4 quantum liquid.[1] The CCM is popular in calculating correlation energies of such systems as atoms, molecules, electron gases, and others in quantum chemistry.[5] However, in the CCM, the ket and bra ground states are not Hermitian to one another[6] and calculations in the CCM are mostly algebraic, very different from those in the CBF method, which relies on determination of distribution functions in real space.

In our earlier papers,[7] by an application to bipartite quantum antiferromagnetic lattice systems, we have extended the CCM to a variational formalism where, in contrast to the traditional CCM, the bra and ket ground states are Hermitian conjugate to one another. Our approach in Ref. 7 is mainly algebraic so an easy comparison with the traditional CCM can be made. In the present paper, we present an alternative scheme based on diagrams. This diagrammatic approach is similar to that in the CBF method. Therefore, a bridge between the CCM and CBF method is built. We organize this paper as follows. In Sec. II, we present a general approach of our method, using the antiferromagnetic lattice model as an example. Section III contains mainly technical parts of our approach. A parallel is made between our approach and that of CBFs. Approximations by resummations and the corresponding results are presented in Sec. IV. Some detailed comparison with the spin-wave theory[8,9] (SWT) is made there. We discuss a possible combination with the CBF method in Sec. V.

II. THE VARIATIONAL COUPLED-CLUSTER METHOD

We take the spin-1/2 antiferromagnetic *XXZ* model on a bipartite lattice as our example. The Hamiltonian is given by

$$H=\frac{1}{2}\sum_{l,\rho}H_{l,l+n}=\frac{1}{2}\sum_{l,n}\left(As_l^zs_{l+n}^z+\frac{1}{2}s_l^+s_{l+n}^-+\frac{1}{2}s_l^-s_{l+n}^+\right), \quad (1)$$

where $A>0$ is the anisotropy constant, the index l runs over all lattice sites, n runs over all z nearest-neighbor sites, and $s^{\pm}$ are the usual spin raising $(+)$ and lowering $(-)$ operators. As $A\to\infty$, the Hamiltonian becomes the classical Ising mode with exact ground state given by the Néel state, a state with two alternating spin-up and -down sublattices. As in our earlier work, we take the Néel state as our model state from which we construct quantum many-body correlations of the ground states. As before, we shall exclusively use the index i for the spin-up sublattice and the index j for the spin-down sublattice. The many-spin correlations in the ground state of Eq. (1) can then be included by considering the excited states with respect to the uncorrelated Néel state. These excited states are constructed by applying the so-called configuration creation operators $C_I^{\dagger}$ to the Néel model state with the nominal index I labeling these operators. In our spin model, the operators $C_I^{\dagger}$ are given by any combination of the spin-flip operators to the Néel state s_i^- and s_j^+; the index I in this case corresponds to the collection of the lattice indices (i's and j's). As discussed in detail in our earlier paper,[7] we use the Coester representation for both the ket and bra ground states and write

$$|\Psi\rangle=e^S|\Phi\rangle,\quad S=\sum_I F_IC_I^{\dagger};\quad \langle\tilde{\Psi}|=\langle\Phi|e^{\tilde{S}},\quad \tilde{S}=\sum_I \tilde{F}_IC_I, \quad (2)$$

where the model state $|\Phi\rangle$ is given by the Néel state as mentioned earlier, and

$$\sum_I F_IC_I^{\dagger}=\sum_{n=1}^{N/2}\sum_{i_1,\ldots,j_1,\ldots}f_{i_1,\ldots,j_1,\ldots}\frac{s_{i_1}^-\cdots s_{i_n}^-s_{j_1}^+\cdots s_{j_n}^+}{(2s)^n} \quad (3)$$

for the ket state with s as spin quantum number and the corresponding Hermitian conjugate of Eq. (3) for the bra state, using the notation $\tilde{F}_I=\tilde{f}_{i_1,\ldots,j_1,\ldots}$ for the bra-state coefficients. The coefficients $\{F_I,\tilde{F}_I\}$ are then determined by the usual variational equations as

$$\frac{\delta\langle H\rangle}{\delta\tilde{F}_I}=\frac{\delta\langle H\rangle}{\delta F_I}=0,\quad \langle H\rangle\equiv\frac{\langle\tilde{\Psi}|H|\Psi\rangle}{\langle\tilde{\Psi}|\Psi\rangle}. \tag{4}$$

We define the so-called bare distribution functions as

$$g_I=\langle C_I\rangle,\quad \tilde{g}_I=\langle C_I^\dagger\rangle, \tag{5}$$

where we have exchanged the definition of g_I with that of $\tilde{g}_I$ as compared with those in Ref. 7 for purely notational reasons. The Hamiltonian expectation $\langle H\rangle$ is shown, in general, to be a function containing up to linear terms in g_I and $\tilde{g}_I$ and a finite-order polynomial in F_I (or in $\tilde{F}_I$) in Eq. (21) of Ref. 7:

$$\langle H\rangle=\mathcal{H}(g_I,\tilde{g}_I,F_I)=\mathcal{H}(\tilde{g}_I,g_I,\tilde{F}_I). \tag{6}$$

Two systematic schemes have been developed for calculating the distribution functions of Eqs. (5): one is algebraic and the other is diagrammatic. In the algebraic approach, by taking advantage of the properties of the operators, it is straightforward to derive the following self-consistent sets of equations for the distribution functions:

$$g_I=G(\tilde{g}_J,F_J),\quad \tilde{g}_I=G(g_J,\tilde{F}_J), \tag{7}$$

where G is a function containing up to linear terms in $\tilde{g}_J$ (or g_J) and a finite-order polynomial in F_J (or $\tilde{F}_J$). We want to point out that Eqs. (2) and (4)–(7) are the main general equations of the variational CCM.

III. DIAGRAMMATIC REPRESENTATION OF GENERATING FUNCTIONAL

In this section, we calculate the bare distribution functions g_I and $\tilde{g}_I$ of Eq. (5) by employing a diagrammatic scheme. As a demonstration, we consider a simple truncation approximation in which the correlation operators S and $\tilde{S}$ of Eqs. (2) retain only the two-spin-flip operators as (the so-called SUB2 approximation as defined in Ref. 10),

$$S\approx\sum_{ij}f_{ij}C_{ij}^\dagger=\sum_{ij}f_{ij}\frac{s_i^-s_j^+}{2s},\quad \tilde{S}\approx\sum_{ij}\tilde{f}_{ij}C_{ij}=\sum_{ij}\tilde{f}_{ij}\frac{s_i^+s_j^-}{2s}. \tag{8}$$

In this approximation, the expectation value of Eq. (1) is given by

$$\langle H_{ij}\rangle=A\langle s_i^zs_j^z\rangle+\frac{1}{2}(g_{ij}+\tilde{g}_{ij}), \tag{9}$$

where $\langle s_i^zs_j^z\rangle$ is calculated as

$$\langle s_i^zs_j^z\rangle=-s^2+s\left(\sum_{i'}\rho_{i'j}+\sum_{j'}\rho_{ij'}\right)-\left(\sum_{i'j'}\rho_{ij',i'j}+\rho_{ij}\right). \tag{10}$$

ρ_{ij} is the usual full one-body distribution function defined as

$$\rho_{ij}\equiv f_{ij}\tilde{g}_{ij}=f_{ij}\frac{\langle s_i^-s_j^+\rangle}{2s}, \tag{11}$$

and $\rho_{ij,i'j'}$ is the full two-body distribution function defined as

$$\rho_{ij,i'j'}\equiv f_{ij}f_{i'j'}\tilde{g}_{ij,i'j'}=f_{ij}f_{i'j'}\frac{\langle s_i^-s_j^+s_{i'}^-s_{j'}^+\rangle}{(2s)^2}. \tag{12}$$

The order parameter is given by

$$\langle s_i^z\rangle=s-\rho, \tag{13}$$

where $\rho=\Sigma_j\rho_{ij}$, taking advantage of translational invariance.

We define a generating functional W in the usual fashion as

$$W\equiv\ln\langle\tilde{\Psi}|\Psi\rangle, \tag{14}$$

so that the bare and full distribution functions can be simply expressed as functional derivatives of W. For example, the one-body and two-body bare functions are given by

$$\tilde{g}_1=\langle C_1^\dagger\rangle=\frac{\delta W}{\delta f_1},\quad \tilde{g}_{12}=\langle C_1^\dagger C_2^\dagger\rangle=\frac{\delta^2W}{\delta f_1\delta f_2}+\tilde{g}_1\tilde{g}_2, \tag{15}$$

where, for simplicity, we have employed the notation $1\equiv(i_1,j_1)$ so that $f_1=f_{i_1j_1}$, etc.; and the structure function S_{12} has the usual relation as in the CBF method as

$$S_{12}\equiv f_1\frac{\delta\rho_2}{\delta f_1}=\rho_1\delta_{12}+\rho_{12}-\rho_1\rho_2, \tag{16}$$

where $\rho_1=\rho_{i_1j_1}$, etc.

We now write W in terms of a linked-cluster expansion:

$$W=(\text{sum of all linked cluster contributions}). \tag{17}$$

The main task of this section is to find a diagrammatic scheme to categorize this expansion. We first expand the ket-state operator in the simplified notation $e^S=1+S+(1/2!)S^2+\cdots=1+f_1C_1^\dagger+(1/2!)f_1f_2C_1^\dagger C_2^\dagger+\cdots$, where in the last equation, the summation over all indices is understood. The normalization integral

$$\langle\tilde{\Psi}|\Psi\rangle=1+\tilde{f}_{1'}f_1\langle C_{1'}C_1^\dagger\rangle+\frac{1}{(2!)^2}\tilde{f}_{2'}\tilde{f}_{1'}f_1f_2\langle C_{2'}C_{1'}C_1^\dagger C_2^\dagger\rangle+\cdots \tag{18}$$

can be evaluated straightforwardly for the first few terms. In the above series, the primed indices are used for bra-state expansion. We notice that each term of Eq. (18) contains an equal number of creation and destruction operators (otherwise, the expectation is zero).

The first-order expectation is easily calculated as $\langle C_{1'}C_1^\dagger\rangle=[1/(2s)^2]\langle\Phi|s_{j_1}^-,s_{i_1}^+,s_{i_1}^-s_{j_1}^+|\Phi\rangle=\delta_{i_1',i_1}\delta_{j_1',j_1}$. Hence we have, writing out the summation explicitly,

$$(\text{first order})=\sum_1 f_1\tilde{f}_1. \tag{19}$$

The calculation of the second-order expectation $\langle C_{2'}C_{1'}C_1^\dagger C_2^\dagger\rangle$ is more complicated. We first consider the case

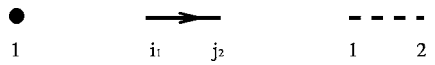

FIG. 1. Three basic elements for construction of diagrams, where simplified index notations $1 \equiv (i_1, j_1)$, etc., are used.

of $1 \neq 2$ (i.e., $i_1 \neq i_2$ and $j_1 \neq j_2$). There are four nonzero terms,

$$(\delta_{i_1 i_1}\delta_{i_2 i_2} + \delta_{i_1 i_2}\delta_{i_2 i_1})(\delta_{j_1 j_1}\delta_{j_2 j_2} + \delta_{j_1 j_2}\delta_{j_2 j_1})$$
$$= (\delta_{i_1 i_1}\delta_{i_2 i_2} + \delta_{i_1 i_2}\delta_{i_2 i_1})(\delta_{j_1 j_1}\delta_{j_2 j_2} + \delta_{j_1 j_2}\delta_{j_2 j_1}).$$

The cases when $i_1 = i_2$ and/or $j_1 = j_2$ can be easily accounted for by introducing a factor involving the usual δ functions as

$$\left(1 - \frac{1}{2s}\delta_{i_1 i_2}\right)\left(1 - \frac{1}{2s}\delta_{j_1 j_2}\right) = 1 + \Delta_{12},$$

with the definition

$$\Delta_{12} \equiv -\frac{1}{(2s)}(\delta_{i_1 i_2} + \delta_{j_1 j_2}) + \frac{1}{(2s)^2}\delta_{i_1 i_2}\delta_{j_1 j_2}. \tag{20}$$

This is because $(s_i^-)^2 = (s_j^+)^2 = 0$ for $s = 1/2$, a manifestation of the Pauli exclusion principle. The second-order contribution is hence derived as

$$\frac{1}{(2!)^2}\tilde{f}_{2'}\tilde{f}_{1'}f_1 f_2(\delta_{i_1 i_1}\delta_{i_2 i_2} + \delta_{i_1 i_2}\delta_{i_2 i_1})(\delta_{j_1 j_1}\delta_{j_2 j_2} + \delta_{j_1 j_2}\delta_{j_2 j_1})$$
$$\times(1 + \Delta_{12}) = \frac{1}{2!}[(f_1\tilde{f}_1)(f_2\tilde{f}_2) + f_1 f_2 \tilde{f}_{i_1 j_2}\tilde{f}_{i_2 j_1}](1 + \Delta_{12}),$$

where the second term inside the square brackets clearly represents the so-called exchange contributions. We wish to point out that we do not need a separate set of δ functions of Eq. (20) for the bra-state operators $C_{n'}$. This is due to the fact that each of the bra-state operators always needs to match one of the ket-state operators in order to give a nonzero contribution in the expansion of Eq. (18). We also notice that the expression of Eq. (20) is in fact also correct for spin quantum number $s > 1/2$ because, for a general s,

$$\frac{1}{2(2s)^2}\langle\Phi|(s_i^+)^2(s_i^-)^2|\Phi\rangle = \left(1 - \frac{1}{2s}\right),$$

etc. For higher-order terms in the expansion of Eq. (18), the extension of the Pauli exclusion principle can be simply written as a product of two-body factors as

$$\prod_{n>m}(1 + \Delta_{nm}). \tag{21}$$

We notice that the above product in general is not exact any more but an approximation for $s > 1/2$, as the three-body effects [e.g., from $(s_{i_1}^-)^3$ when $i_1 = i_2 = i_3$] have been ignored.

In order to extend to higher-order calculations including the exchange contributions, we need a systematic graph representation. For this purpose, as shown in Fig. 1, we use a solid dot to represent the ket-state coefficient f_1 with $1 = (i_1 j_1)$ as defined earlier; a (directed) exchange line drawn from i_1 to j_2 to represent the bra-state coefficient $\tilde{f}_{i_1 j_2}$; and a Pauli (dashed) line drawing between any two dots to represent the δ function Δ_{12} of Eq. (20). With these graphic notations, a linked contribution is represented by a connected diagram. After detailed calculations up to fifth order, we have established the following simple and complete rules for construction of these diagrams in the normalization integral of Eq. (18): (1) The kth-order contribution consists of all possible diagrams involving k dots; (2) in each diagram the number of dots is equal to the number of exchange lines; (3) A dot is always connected by exchange lines (leaving and coming) and hence exchange lines always form loops; (4) between any pair of dots one can draw at most one Pauli line; (5) the contribution of each diagram is divided by its symmetry factor; and (6) summations over all indices are involved.

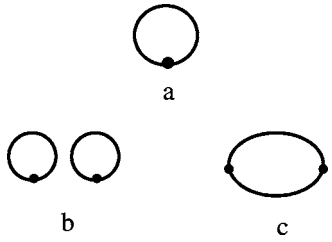

FIG. 2. First- and second-order contributions in the expansion of Eq. (18).

We first consider the case without any Pauli line, $\Delta_{nm} = 0$. (This is equivalent to turning spin operators to boson operators as will be shown later.) For example, the first-order contribution of Eq. (19) is simply a dot with an exchange line leaving and coming as shown as diagram a in Fig. 2, where the direction of the exchange line is clockwise as in most other diagrams (we therefore do not show the arrows of exchange lines explicitly). The second-order contribution with $\Delta_{12} = 0$ is given by the two diagrams b and c in Fig. 2, namely, $(1/2!)(b+c)$. The third-order contribution is calculated as $(1/3!)(a+3b+2c)$ and is shown in Fig. 3, where the factor 3 for diagram b is due to the three equivalent diagrams by rotation, and the factor 2 for diagram c comes from the two equivalent diagram with opposite directions, one clockwise the other counterclockwise (this is referred to as parity symmetry). In similar fashion one can write down the fourth-order contribution as shown in Fig. 4 for the corresponding diagrams as

$$(\text{fourth order}) = \frac{1}{4!}(a + 6b + 8c + 3d + 6e), \tag{22}$$

where the coefficient numbers are the symmetry factors of the corresponding diagrams. For example, the factor 6 for

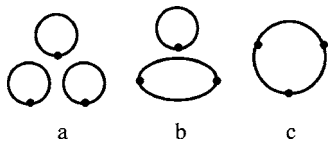

FIG. 3. Diagrams of third-order contributions in the expansion of Eq. (18).

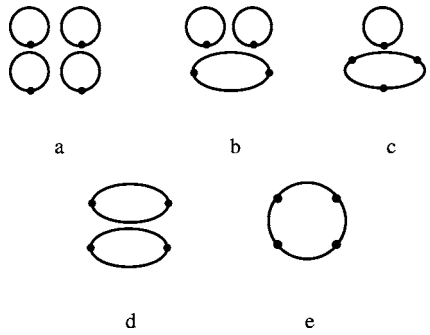

FIG. 4. Similar to Fig. 3 but for the fourth-order contributions.

diagram e is due to the fact that there are three equivalent diagrams each with parity symmetry factor of 2. The fifth-order contributions include seven independent diagrams, as shown in Fig. 5, namely,

$$(\text{fifth order}) = \frac{1}{5!}(a + 10b + 20c + 15d + 30e + 20f + 24g). \tag{23}$$

We notice that, in all these results, the last term represents a ring diagram with k dots in the kth-order contribution. We use R_k to represent this ring diagram with the symmetry factor $(k-1)!/k! = 1/k$. For example, the fourth-order ring contribution is, writing out the summations explicitly,

$$R_4 = \frac{1}{4}\sum_{1,2,3,4} f_1 \tilde{f}_{i_1 j_2} f_2 \tilde{f}_{i_2 j_3} f_3 \tilde{f}_{i_3 j_4} f_4 \tilde{f}_{i_4 j_1}. \tag{24}$$

Furthermore, the other terms in these k-order contributions are simply a product of smaller ring contributions. This property can be extended to higher order. (For this purpose one needs to apply the symmetric group $\mathcal{S}_n$ to count the number of diagrams. See, for example, Ref. 11.) We are now in position to write all contributions without any Pauli line in terms of these ring diagrams. The normalization integral of Eq. (18) is then written as

$$\langle\tilde{\Psi}|\Psi\rangle_{\Delta_{nm}=0} = \sum_{k=0}^{\infty} {\sum_{\nu_1 \cdots \nu_k}}' \frac{1}{k!}\frac{1}{\nu_1!}(R_1)^{\nu_1}\frac{1}{\nu_2!}(R_2)^{\nu_2}\cdots\frac{1}{\nu_k!}(R_k)^{\nu_k}$$
$$= \exp(R_1 + R_2 + R_3 + \cdots),$$

where the prime in Σ' implies the restriction $1\nu_1 + 2\nu_2 + \cdots + k\nu_k = k$. The corresponding generating functional W' without any Pauli line is simply

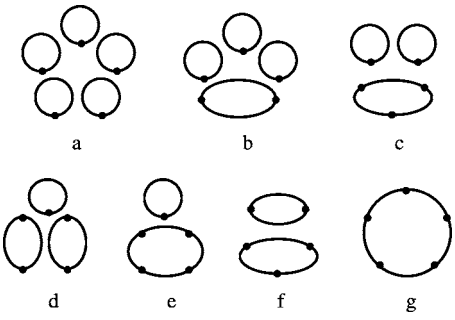

FIG. 5. Similar to Fig. 3 but for the fifth-order contributions.

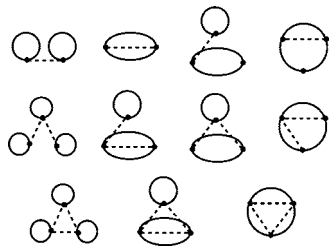

FIG. 6. Diagrams of up to third-order contributions to the generating functional W of Eq. (26) except ring diagrams R_1, R_2, R_3. The corresponding symmetry factors are, in the same order as the list of diagrams, $(1/2, 1/2, 1, 1, 1/2, 1, 1/2, 1, 1/3!, 1/2, 1/3)$.

$$W' \equiv W|_{\Delta_{nm}=0} = \sum_{k=1}^{\infty} R_k. \tag{25}$$

To include Pauli lines (i.e., $\Delta_{nm} \neq 0$), we use the notation L_k to represents the contribution of all linked k-clusters and write

$$W = \ln\langle\tilde{\Psi}|\Psi\rangle = L_1 + L_2 + L_3 + \cdots. \tag{26}$$

Using the simple rules discussed earlier, without much difficulty, we can list all k-cluster contributions of L_k in terms of a ring diagram R_k plus all possible ways of drawing Pauli lines between any pair of k dots of rings, including those pairs of dots between rings and those pairs of dots inside rings. In Fig. 6 we list all contributions up to third order except R_1, R_2, and R_3.

IV. DIAGRAM RESUMMATIONS, SPIN-WAVE THEORY, AND BEYOND

We first consider all diagrams without any Pauli line, namely, all the ring diagram contributions R_k with $k = 1, 2, \ldots$, and show that the spin-wave theory is thus reproduced. As can be seen from Eq. (20), these ring diagrams represent the first-order approximation in the large-s limit. In fact, in this limit, operators s_i^- and s_j^+ behave like bosons as $s_i^- \to \sqrt{2s}a_i^\dagger$, $s_j^+ \to \sqrt{2s}b_j^\dagger$.[8,9] The corresponding wave function by Eq. (8) becomes the spin-wave function

$$|\Psi\rangle \to |\Psi_{sw}\rangle = \exp\left(\sum_{ij} f_{ij} a_i^\dagger b_j^\dagger\right)|\Phi\rangle = \prod_q \exp(f_q a_q^\dagger b_{-q}^\dagger)|\Phi\rangle, \tag{27}$$

where the Néel state $|\Phi\rangle$ should be considered as the vacuum state for the two sets of bosons $a_i^\dagger$ and $b_j^\dagger$ and where, in the last equation, we have made Fourier transformations using the translational symmetry as

$$a_i^\dagger = \sqrt{\frac{2}{N}}\sum_{\mathbf{q}} e^{-i\mathbf{q}\cdot\mathbf{r}_i} a_q^\dagger, \quad b_j^\dagger = \sqrt{\frac{2}{N}}\sum_{\mathbf{q}} e^{-i\mathbf{q}\cdot\mathbf{r}_j} b_q^\dagger,$$

FIG. 7. The ring expansion of the one-body bare distribution function $\tilde{g}_1$ of Eq. (31).

$$f_{ij} = \frac{2}{N}\sum_{\mathbf{q}} e^{-i\mathbf{q}\cdot(\mathbf{r}_j-\mathbf{r}_i)} f_q,$$

with summation over $\mathbf{q}$ restricted to the magnetic zone. The normalization integral of Eq. (27) can be easily calculated as the wave function is uncoupled in q space. Using the expansion $\exp(f_q a_q^\dagger b_{-q}^\dagger) = \Sigma_n (f_q a_q^\dagger b_{-q}^\dagger)^n / n!$ and the simple algebra $\langle \Phi | a_q^n (a_q^\dagger)^n | \Phi \rangle = n!$, we have the following well-known result (see, for example, Chapter 2 of Ref. 12):

$$\langle \Psi_{sw} | \Psi_{sw} \rangle = \prod_q \frac{1}{1 - \tilde{f}_q f_q}. \tag{28}$$

The corresponding generating functional is hence given by

$$W_{sw} = \ln \langle \Psi_{sw} | \Psi_{sw} \rangle = -\sum_q \ln(1 - \tilde{f}_q f_q)$$

$$= \sum_q \left(\tilde{f}_q f_q + \frac{1}{2} (\tilde{f}_q f_q)^2 + \cdots \right), \tag{29}$$

which is precisely the result of Eq. (25) after Fourier transformation, namely,

$$W' = W_{sw}. \tag{30}$$

Distribution functions without any Pauli line can be easily calculated using the functional derivatives of Eqs. (15) and (16) with diagrammatic representation. For example, the one-body bare distribution function $\tilde{g}_1' = \delta W' / \delta f_1$ is simply represented by Fig. 7, where the action of the partial derivative is equivalent to unfolding the ring. Writing out the summations explicitly, we have the expansion of Fig. 7 as

$$\tilde{g}_1' = \tilde{f}_1 + \sum_2 \tilde{f}_{i_1 j_2} f_2 \tilde{f}_{i_2 j_1} + \sum_{2,3} \tilde{f}_{i_1 j_2} f_2 \tilde{f}_{i_2 j_3} f_3 \tilde{f}_{i_3 j_1} + \cdots, \tag{31}$$

and a similar expansion for g_1'. A close inspection of the $\tilde{g}_1'$ and g_1' expansions yields the self-consistency equations

$$\tilde{g}_1' = \tilde{f}_1 + \sum_2 \tilde{f}_{i_1 j_2} g_2' \tilde{f}_{i_2 j_1}, \quad g_1' = f_1 + \sum_2 f_{i_1 j_2} \tilde{g}_2' f_{i_2 j_1}, \tag{32}$$

agreeing exactly with Eq. (31) of Ref. 7 in this SWT approximation. The two-body functions in this approximation can also be easily obtained in this fashion as given in Ref. 7. The spontaneous magnetization of Eq. (13) is given by $\langle s_i^z \rangle = s - \rho'$, with ρ' given by

$$\rho' = \sum_j \rho_{ij}' = \sum_q \frac{\tilde{f}_q f_q}{1 - \tilde{f}_q f_q} = \frac{1}{2} \sum_q \left(\frac{1}{\sqrt{1 - \gamma_q^2 / A^2}} - 1 \right), \tag{33}$$

where we have used the reproduced SWT results of Ref. 7,

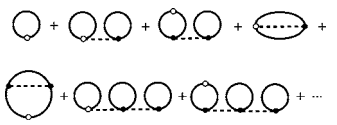

FIG. 8. First few contributions to the full one-body distribution function ρ_1 of Eq. (35), where open dots indicate no summations over its indices while solid dots indicate such summations as before.

$$\tilde{f}_q = f_q = \frac{A}{\gamma_q} (\sqrt{1 - \gamma_q^2 / A^2} - 1), \quad \gamma_q = \frac{1}{z} \sum_n e^{i\mathbf{q}\cdot\mathbf{r}_\mathbf{n}}, \tag{34}$$

where z is the coordination number and n is the nearest-neighbor index of the bipartite lattice. For a one-dimensional (1D) model at the isotropic point $A=1$, the integral of Eq. (33) diverges, in contrast to the well-known exact result of $\rho = 1/2$ for $s = 1/2$ by the Bethe ansatz (see Ref. 10 for references).

To go beyond the SWT, we need to include Pauli lines. Using a similar resummation technique as discussed above, we express the expansion of the bare one-body distribution function $\tilde{g}_1$ in terms of diagrams as shown in Fig. 8, similar to the expansion in Chap. 9 of Ref. 12 and in Ref. 13, after multiplying f_1 on both sides of the equation,

$$\rho_1 = f_1 \tilde{g}_1 = f_1 \frac{\delta W}{\delta f_1} = (\text{Fig. 8}), \tag{35}$$

where we have done all resummations of ring diagrams as in Eq. (31) and hence all exchange lines in the diagrams of Fig. 8 are now functions $\tilde{g}_{ij}'$, not the original exchange line functions $\tilde{f}_{ij}$. As a start, we consider the simplest approximation which contains only the first two diagrams of Fig. 8 (the first one being SWT) as

$$\rho_1 \approx \rho_1' + \rho_1' \sum_2 \Delta_{12} \rho_2'. \tag{36}$$

After summing over the index j_1 with $\rho = \Sigma_{j_1} \rho_{i_1 j_1}$, we have, using Eq. (20) for Δ_{12},

$$\rho = \rho' - \frac{2}{2s} (\rho')^2 + \frac{1}{(2s)^2} \sum_j (\rho_{ij}')^2. \tag{37}$$

For $s = 1/2$ and isotropic point $A=1$, we obtain $\rho \approx 0.127$ for the square lattice and 0.067 for the cubic lattice. They are smaller than $\rho' = 0.197$ and 0.078 of the SWT, respectively. This is not surprising because SWT is known to have overestimated the quantum fluctuations. The best numerical values for the square lattice are around $\rho = 0.16$, including results from extrapolation of high-order localized CCM calculations.[14] For the 1D isotropic model, however, ρ of Eq. (37) diverges as ρ' diverges as mentioned earlier.

We next consider an approximation involving higher-order Pauli lines by including all higher-order diagrams similar to that of Eq. (36), as shown in Fig. 9. This infinite series can again be resummed in a closed form as a self-consistency equation, equivalent to replacing ρ_2' in Eq. (36) by ρ_2 itself as

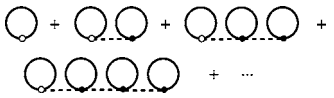

FIG. 9. Super-ring diagram expansion, similar to the ring diagram expansion of Fig. 7 but now involving Pauli lines and with resummations of ring diagrams already carried out in all exchange lines. See text for more details.

$$\rho_1 = \rho_1' + \rho_1' \sum_2 \Delta_{12}\rho_2. \tag{38}$$

The resummation in Eq. (38) is similar to the resummation of rings in Eqs. (31) and (32); we therefore refer to it as the super-ring resummation. The numerical results for ρ thus obtained at the isotropic point for high dimensions improve slightly, as $\rho=0.145$ for the square lattice and 0.068 for the cubic lattice. The square-lattice result compares well to the best results of about 0.16 by other high-order, computation-intensive calculations mentioned earlier (see Ref. 14 and references therein).

For the 1D model, Eq. (38) can be easily expressed as

$$\rho = \frac{B}{1+2B/2s}, \quad B \equiv 2\sum_{r=0}^{\infty} \frac{\rho_r'}{1-\rho_r'/(2s)^2}, \tag{39}$$

where $\rho_r' = f_r \tilde{g}_r$ is the one-body distribution function in real space and Eq. (33) is simply $\rho' = 2\Sigma_r f_r \tilde{g}_r$ in this equivalent expression with

$$f_r = \frac{1}{\pi}\int_0^{\pi} dq \cos(2r+1)f_q, \quad r = 0,1,2, \ldots, \tag{40}$$

and similarly for $\tilde{g}_r$. The Fourier functions f_q and $\tilde{g}_q$ are given by Eqs. (33) and (34). At the isotropic Heisenberg point $A=1$ and for $s=1/2$, Eq. (39) produces a convergent, precise number $\rho=1/2$ due to the divergence of ρ' and B. This is interesting indeed as the divergence of SWT has troubled theorists for many years. For $A>1$, numerical results can be easily calculated using these equations. We wish to point out that SWT also produces unphysical results with the negative order parameter of Eq. (13) for $A<1.05$ while our results for the order parameter are all positive, right down to $A=1$ where our result for the order parameter is precisely zero as mentioned. But the essential singularity of the exact results in the region close to $A=1$ (see Ref. 10) is not reproduced. This is not surprising as our wave functions retain only two-spin-flip approximations as given by Eqs. (8). Our 1D result for $A>1.1$ is not much different from that of SWT. It is worth mentioning that the traditional CCM SUB2 approximation[15] also produced a convergent result for the 1D model but at $A=0.37$, not the isotropic point $A=1$.

For $A<1$, the Hamiltonian of Eq. (1) describes different states with qualitatively different properties. It is beyond the scope of our present paper as different model state(s) from the Néel state as used here would be more suitable. We also leave calculations including other higher-order terms and resummations in the two-body function ρ_{12} and structure function S_{12} of Eq. (16) for consideration elsewhere.

V. DISCUSSION

In this paper, we present a diagrammatic scheme for the calculations of distribution functions of the variational CCM, as an alternative to the algebraic scheme published in our earlier papers.[7] The results of SWT are reproduced by an approximation which resums all ring diagrams without any Pauli line. Approximations beyond the SWT can also easily be made by including diagrams with Pauli lines. One such approximation, which includes all super-ring diagrams by a resummation of infinite Pauli lines in addition to resummations of all ring diagrams, produces a convergent, precise number for the order parameter of the 1D isotropic model, in contrast to the divergence of SWT. This cure of SWT divergence is also interesting to 2D models (including square and triangle lattices) as naive higher-order calculations within the framework of SWT are also likely to produce divergent results, despite the fact that the first-order results are reasonable. We believe that similar resummations of super-ring diagrams as Fig. 9 and Eq. (38) may provide a solution for such divergence problems. We leave more detailed calculations for consideration elsewhere.

It is also possible to include in the ground state higher-order many-body correlations such as four-spin-flip operators, in additional to the two-spin-flip operators of Eqs. (8). Furthermore, as demonstrated here by the diagrammatic approach, a direct link between our variational CCM and the powerful CBF method has now been established, as both rely on determination of distribution functions through functional derivatives of a generating functional. In particular, as given by Eq. (13), the particle density ρ in CBF is equivalent to the order parameter of our spin models as $\langle s_i^z \rangle = s - \rho$. Its diagrammatic expansions in the two theories are similar (see Chap. 9 of Ref. 12 and Ref. 13 for more CBF details). For 2D and 3D lattice models, the values of density ρ are small compared with s. Such spin systems can therefore be described as dilute gases (dilute gases of quasiparticle magnons of spin waves). For the isotropic 1D model, the density ρ is *saturated*, corresponding to the order parameter equal to zero, a critical value. Our approximation including a resummation of super-ring diagrams is capable of reproducing precisely this saturation number. It is also interesting to know that our diagrammatic analysis of the variational CCM is for the translational invariance lattice system while a similar analysis in the CBF method is for inhomogeneous systems.[12,13]

For more accurate results in general, we need to include correlations between those quasiparticles in our ground state, and the CBF method is well known to be one of the most effective theories for dealing with such particle correlations (even when they are very strong as in a helium-4 quantum liquid[1]) by systematic calculations of the important two-body distribution functions. We therefore propose a unified trial wave function $|\Psi_U\rangle$ as, including a generalized Jastrow correlation operator S^0 involving the quasiparticle density operator s^z,

$$|\Psi_U\rangle = e^{S^0/2}|\Psi\rangle, \quad S^0 = \sum_{ij} f_{ij}^0 s_i^z s_j^z, \tag{41}$$

where $\{f_{ij}^0\}$ are the additional variational parameters and $|\Psi\rangle$ is our variational CCM state of Eq. (2). The diagrammatic

scheme as discussed in this paper is useful for calculating the expansion of the generating functional of Eq. (41). We have made progress in such calculations and wish to report results soon. We also believe such a unified many-body theory may prove to be capable of dealing with strongly correlated fermion systems in general.

ACKNOWLEDGMENTS

I am grateful to R. F. Bishop for introducing the CCM to me. Useful discussions with J. Arponen, R. F. Bishop, F. Coester, and H. Kümmel are also acknowledged.

[1] J. W. Clark and E. Feenberg, Phys. Rev. **113**, 388 (1959); E. Feenberg, *Theory of Quantum Fluids* (Academic Press, New York, 1969).

[2] J. Hubbard, Proc. R. Soc. London, Ser. A **240**, 539 (1957); A. Hugenholtz, Physica (Amsterdam) **23**, 481 (1957); **23**, 533 (1957); F. Coester, Nucl. Phys. **7**, 421 (1958).

[3] F. Coester and H. Kümmel, Nucl. Phys. **17**, 477 (1960).

[4] J. Čižek, J. Chem. Phys. **45**, 4256 (1966); Adv. Chem. Phys. **14**, 35 (1969).

[5] R. F. Bishop, Theor. Chim. Acta **80**, 95 (1991); R. J. Bartlett, *ibid.* **80**, 71 (1991).

[6] J. Arponen, Ann. Phys. (N.Y.) **151**, 311 (1983).

[7] Y. Xian, in 150 *Years of Quantum Many-Body Theories*, edited by R. F. Bishop, K. A. Gernoth, and N. R. Walet (World Scientific, Singapore, 2001), p. 107; Y. Xian, Phys. Rev. B **66**, 184427 (2002).

[8] P. W. Anderson, Phys. Rev. **86**, 694 (1952).

[9] M. Takahashi, Phys. Rev. B **40**, 2494 (1989).

[10] B. F. Bishop, J. B. Parkinson, and Y. Xian, Phys. Rev. B **43**, R13782 (1991); **44**, 9425 (1991).

[11] M. Hammermesh, *Group Theory* (Addison-Wesley, Reading, MA, 1962), Chap. 1.

[12] J.-P. Blaiza and G. Ripka, *Quantum Many-Body Theory of Finite Systems* (MIT Press, London, 1986).

[13] E. Krotscheck, Phys. Rev. B **31**, 4267 (1985).

[14] R. F. Bishop, R. G. Hale, and Y. Xian, Phys. Rev. Lett. **73**, 3157 (1994); Chen Zeng, D. J. J. Farnell, and R. F. Bishop, J. Stat. Phys. **90**, 327 (1998).

[15] R. F. Bishop, J. B. Parkinson, and Y. Xian, Phys. Rev. B **46**, 880 (1992).